



## Influence of sugarcane bagasse ash substitution on Portland cement characteristics

Darweesh HHM<sup>1</sup>✉, Abo El-Suoud MR<sup>2</sup>

<sup>1</sup>Refractories, Ceramics and Building Materials Department, National Research Centre, Cairo, Egypt

<sup>2</sup>Botany Department, National Research Centre, Cairo, Egypt

### ✉Correspondence author

Refractories, Ceramics and Building Materials Department, National Research Centre, Cairo, Egypt

Email: hassandarweesh2000@yahoo.com

### Article History

Received: 20 June 2019

Accepted: 07 August 2019

Published: August 2019

### Citation


Darweesh HHM, Abo El-Suoud MR. Influence of sugarcane bagasse ash substitution on Portland cement characteristics. *Indian Journal of Engineering*, 2019, 16, 252-266

### Publication License



© The Author(s) 2019. Open Access. This article is licensed under a [Creative Commons Attribution License 4.0 \(CC BY 4.0\)](https://creativecommons.org/licenses/by/4.0/).

### General Note

 Article is recommended to print as color digital version in recycled paper.

### ABSTRACT

The results showed that as the bagasse ash content (BA) increased, the fineness of mixes and heat of hydration increased too. Water of consistency and setting times decreased with BA content due to the presence of Na-lignosulphonate superplasticizer. Combined water content improved and enhanced up to 28 days of hydration and then seemed to be nearly constant. The bulk density and compressive strength increased while apparent porosity decreased up to 12 % BA addition and then decreased onward, whereas apparent porosity increased. So, > 12 % BA content, all properties evidently declined. Free lime content of B0 increased up to 90 days due to the normal hydration of C<sub>3</sub>S and β-C<sub>2</sub>S phases of the cement, but increased only up to 3 days with incorporation of BA and then decreased onward. FTIR spectra showed a large amount of free lime with B0, but it decreased in presence of BA. SEM microscopy showed the formation of ettringite phase as needle-like crystals and sheets or aggregate of CSH and/or CAH.

**Keywords:** OPC; sugarcane bagasse ash; setting times; strength; FTIR; SEM

## 1. INTRODUCTION

### Scope of the problem

The necessity to utilize waste materials (solids, liquids or even gases), and to decrease the overall energy consumption is becoming increasingly obvious. The benefits from applying pozzolanic materials as fly ash, rice husk ash, palm oil ash and fuel ash as a partial replacement of Portland cement in concrete are well established. These pozzolanic materials can improve workability, strength and durability of cement and/or concrete [1-7]. It is well known that sugarcane is the main food crop in tropical and subtropical countries because it is considered as the major resource for sugar production and also the sugar industry plays a vital part in the countrywide economy of any country.

Sugarcane bagasse (SCB) is a solid waste material that created after the extraction of juice from sugarcane. Generally, the bagasse waste is disposed to the landfills or disposal sites so that it now represents a heavy environmental burden. Furthermore, the SCB creates an environmental nuisance due to the direct disposal on the open areas so that it can form garbage heaps in these areas [1, 6, 8]. Barroso [9] stated that one ton from sugarcane could generate 280 kg of bagasse waste. There are huge quantities of sugar are produced worldwide. Therefore, the solid waste of bagasse coming from sugar industry is nearly about 40-45 %. Hence, the annual discard of bagasse is about 600 million tons [10, 11]. To reduce the environmental burden of this SCB, the utilization of this waste material in cement pastes, mortars or even concrete is a significant aspect. The burning of organic wastes, like SCB, produces a considerable amount of ash [12, 13]. One of the effective ways to reduce the environmental impact is to use it as a mineral admixture for the partial replacement of cement in concrete, which will have the possibility to reduce the cost production, energy conservation, and waste emission [14, 15]. The sugarcane bagasse ash (SBA) is acquired through the control burning of SCB. Bagasse ash (BA) could be used as a partial replacement in concrete because it contains amorphous silica, which has pozzolanic properties [8-12]. In addition, Kawade [16] has carried out the research work on SBA as a partial replacement of cement with 10, 15, 20, 25 and 30 wt. % cement replacement of concrete. He found that the OPC could favorably be replaced with (BA) only 10%.

### Objective of the current study

In the present work, the authors tried to utilize a larger amount of BA in the Portland cement pastes as a pozzolanic material than used before. The physical properties, w/c ratio, setting times, chemically-bound water and free lime contents, bulk density, apparent porosity and compressive strength were investigated. The obtained results would be confirmed with FTIR and SEM spectroscopy.

## 2. EXPERIMENTAL AND METHODS

### Raw materials

The used raw materials in the current research article are Ordinary Portland cement (OPC Type I- CEM I 42,5R) with Blaine surface area 3400 cm<sup>2</sup>/g, and sugarcane bagasse (SCB) as a source of nanosilica with a fineness of 300 μm. The OPC was supplied from Sakkara cement factory, Giza, Egypt, and its commercial name is known as "Asmant El-Momtaz", while SCB sample was provided by sugarcane juice shops, Egypt. The SCB was first processed and washed with running water, and also with distilled water and then let to dry under sun and open air for few days. The dried SCB was subjected for firing at 650 °C for two hours soaking to produce what is known as Baggasse ash (BA). Then, the resulting BA was screened to pass through 300 μm standard sieve. The chemical composition of the OPC and BA is shown in Table 1. The mineralogical phase composition of the used OPC as calculated from Bogue equations [17, 18] is given in Table 2, while the mix composition is illustrated in Table 3. The BA particles are amorphous and crystalline and it is mainly composed of a large percentage of nano-SiO<sub>2</sub> and a lower percentage of nano-Al<sub>2</sub>O<sub>3</sub>.

### Physical properties

The physical properties [20, 21] of the OPC and BA are calculated from the following relations:

$$K_b = \text{CaO} + \text{MgO} / \text{SiO}_2 + \text{Al}_2\text{O}_3 \quad (1)$$

$$H_m = \text{CaO} / \text{SiO}_2 + \text{Al}_2\text{O}_3 + \text{Fe}_2\text{O}_3 \quad (2)$$

$$S_m = \text{SiO}_2 / \text{Al}_2\text{O}_3 + \text{Fe}_2\text{O}_3 \quad (3)$$

$$A_m = \text{Al}_2\text{O}_3 / \text{Fe}_2\text{O}_3 \quad (4)$$

$$L_m = 100 \times \text{CaO} / 2.8 \times \text{SiO}_2 + 1.1 \times \text{Al}_2\text{O}_3 + 0.7 \times \text{Fe}_2\text{O}_3 \quad (5)$$

where, Kb, Hm, Sm, Am and Lm are the basicity coefficient, hydration modulus, SiO<sub>2</sub> modulus, Al<sub>2</sub>O<sub>3</sub> modulus and CaO modulus, respectively.

**Table 1** Composition of the used raw materials, mass %

Oxide Material	SiO <sub>2</sub>	Al <sub>2</sub> O <sub>3</sub>	Fe <sub>2</sub> O <sub>3</sub>	CaO	MgO	SO <sub>3</sub>	Na <sub>2</sub> O	K <sub>2</sub> O	LOI	Specific gravity
OPC	21.78	4.13	3.15	61.11	2.16	2.78	0.11	0.65	0.87	3.14
BA	70.83	9.21	1.95	8.16	1.32	1.47	0.12	1.65	6.91	2.23

**Table 2** Mineralogical composition of the used OPC sample, mass %

Phase Material	C <sub>3</sub> S	β-C <sub>2</sub> S	C <sub>3</sub> A	C <sub>4</sub> AF
OPC	43.01	30.00	5.65	9.58

**Table 3** The batch composition of cement mixers, mass %

Batch Material	B0	B1	B2	B3	B4	B5	Fineness, cm <sup>2</sup> /g
OPC	100	96	92	88	84	80	3400
BA	----	4	8	12	16	20	6500
Fineness, cm <sup>2</sup> /g	3400	3850	4100	4450	4780	5050	

### Preparation and methods

There are 6 cement batches from OPC and BA as 100:0, 96:4, 92:8, 88:12, 84:16 and 80:20 having the symbols: B0, B1, B2, B3, B4 and B5, respectively. The blending process of the various cement blends was done in a porcelain ball mill using three balls for two hours to assure the complete homogeneity of all cement blends. During casting, a definite percentage of sodium lignosulphonate superplasticizer (Figure 1) was added to the prepared cement mixes in order to avoid the agglomeration of the nanoparticles of the used BA or OPC. Sodium lignosulfonate superplasticizer (SL) was applied due to its higher active than other conventional ones. Its molecular weight is 534.51, while its molecular formula is C<sub>20</sub>H<sub>24</sub>Na<sub>2</sub>O<sub>10</sub>S<sub>2</sub>. It contains several free carboxylic groups which help greatly to improve cement dispersion [17, 16].

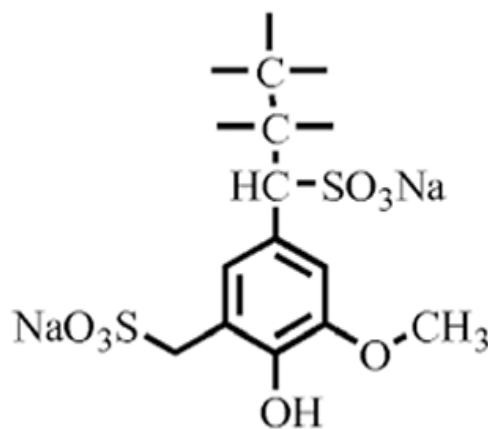


**Figure 1** The chemical structure of sodium lignosulphonate.

The standard water of consistency (WC) as well as setting time (initial and final) of the various cement pastes were directly determined using Vicat Apparatus [22, 23] from the following relation:

$$WC, \% = A / C \times 100 \quad (5)$$

Where, A is the amount of water taken to produce a suitable paste, C is the amount of cement mix (300 g).

The cement pastes were then cast using the predetermined water of consistency, moulded into one inch cubic stainless steel moulds ( $2.5 \times 2.5 \times 2.5 \text{ cm}^3$ ) using about 500 g cement mix, vibrated manually for three minutes and then on a mechanical vibrator for another three minutes. The surface of the moulds was smoothed using a suitable spatula. Thereafter, the moulds were kept in a humidity chamber for 24 hours under  $95 \pm 1 \text{ RH}$  and room temperature, demoulded in the following day and soon cured in water till the time of testing at 1, 3, 7, 28 and 90 days. The bulk density (BD) and apparent porosity (AP) of the hardened cement pastes [18, 24-26] were calculated from the following equations:

$$\text{B. D. (g/cm}^3\text{)} = W_1/(W_1 - W_2) \times 1 \quad (6)$$

$$\text{A. P, \%} = (W_1 - W_3)/(W_1 - W_2) \times 100 \quad (7)$$

Where,  $W_1$ ,  $W_2$  and  $W_3$  are the saturated, suspended and dry weights, respectively.

The compressive strength (CS) of the various hardened cement pastes [27] was measured as follows:

$$\text{CS} = L \text{ (KN)}/S_a \text{ (cm}^2\text{)} \text{ KN/m}^2 \times 102 \text{ (Kg/cm}^2\text{)}/10.2 \text{ (MPa)} \quad (8)$$

Where  $L$  is the load taken,  $S_a$  is the surface area.

Thereafter, about 10 grams of the broken specimens were first well ground, dried at  $105^\circ\text{C}$  for 30 min. and then were placed in a solution mixture of 1:1 methanol: acetone to stop the hydration [28, 29]. The kinetics of hydration in terms of chemically bound water and free lime contents were also measured. About one gram of the sample was first dried at  $105^\circ\text{C}$  for 24h and then the bound water content [4,28,30] at each hydration age was determined on the basis of ignition loss at  $1000^\circ\text{C}$  for 30 min. as follows: About 10 grams of the broken specimens from the determination of compressive strength were first well ground, dried at  $105^\circ\text{C}$  for 30 min. and then were placed in a solution mixture of 1:1 methanol: acetone to stop the hydration [18,28]. The kinetics of hydration in terms of chemically combined water and free lime contents were also measured. About one gram of the sample was first dried at  $105^\circ\text{C}$  for 24h and then the chemically-combined water content ( $\text{CW}_n$ ) at each hydration age was determined on the basis of ignition loss at  $1000^\circ\text{C}$  for 30 min. [28-30] as follows:

$$\text{CW}_n, \% = W_1 - W_2/W_2 \times 100 \quad (9)$$

Where,  $\text{CW}_n$ ,  $W_1$  and  $W_2$  are combined water content, weight of sample before and after ignition, respectively.

The free lime content ( $\text{FL}_n$ ) of the hydrated samples pre-dried at  $105^\circ\text{C}$  for 24h was also determined. About 0.5g sample +40 ml ethylene glycol  $\rightarrow$  heating to about 20 minutes without boiling. About 1–2 drops of pH indicator were added to the filtrate and then titrated against freshly prepared 0.1N HCl until the pink colour disappeared. The 0.1 N HCl was prepared using the following equation: Where,  $W_n$ ,  $W_1$  and  $W_2$  are combined water content, weight of sample before and after ignition, respectively. The free lime content of the hydrated samples pre-dried at  $105^\circ\text{C}$  for 24h was also determined. About 0.5 g sample + 40 ml ethylene glycol  $\rightarrow$  heating to about 20 minutes without boiling. About 1–2 drops of pH indicator were added to the filtrate and then titrated against freshly prepared 0.1 N HCl until the pink colour disappeared. The 0.1 N HCl was prepared using the following equation:

$$V_1 = N \times V_2 \times W(7) \times 100/D \times P \times 1000 \quad (10)$$

Where,  $V_1$  is the volume of HCl concentration,  $V_2$  is the volume required,  $N$  is the normality required,  $W$  is the equivalent weight,  $D$  is the density of HCl concentration and  $P$  is the purity (%).

The heating and titration were repeated several times until the pink colour did not appear on heating. The free lime content [18, 26, 31, 32] was calculated from the following relation:

$$\text{FL}_n, \% = (V \times 0.0033/1) \times 100 \quad (11)$$

Where,  $\text{FL}_n$  and  $V$  are the free lime content and the volume of 0.1 N HCl taken on titration, respectively.

The obtained results were confirmed by infrared spectroscopy (FT-IR) and Scanning Electron Microscopy (SEM). The FT-IR spectra were performed by Perkin Elmer FT-IR spectrometer in the range of 4000-500  $\text{cm}^{-1}$  and a resolution of 500  $\text{cm}^{-1}$ . The SEM images were done for some selected samples by using JEOL-JXA-840 electron analyzer at accelerating voltage of 30 KV. The fractured surfaces were fixed on Cu- $\alpha$  stubs by carbon paste and then coated with a thin layer of gold.

### 3. RESULTS AND DISCUSSION

#### Physical Properties

To specify the type of the used materials in this research work and to identify whether the used BA is recommended by standards and documents or not, the physical properties of the used BA must be studied. On this basis, the physical properties of the used OPC and BA samples are listed in Table 4, and plotted in Figure 2. As it is obvious, the basicity coefficient (Kb) and hydration modulus (Hm) of either OPC or BA samples are almost the same, whereas silica modulus (Sm) and alumina modulus (Am) of BA are much higher than those of OPC. But the lime modulus of OPC is higher than that of BA. The relationship between the Blaine surface area, density and specific gravity of the used OPC and BA samples is represented in Figure 3. The surface area or fineness of BA is higher than that of OPC, while the density is lower. This is mainly due to the siliceous and spongy nature of BA particles which make it light in weight [1-8]. It has been reported that the particles of BA are spongy, which are associated with partially burnt fragments of coal that was resulting from the incomplete combustion. BA often burns at a temperature range of 600–800  $^{\circ}\text{C}$  and so, the sponge-like shape particles are obtained. This is attributed to the lower temperature below the melting point of BA [32, 33]. The data shown in Tables 3 and 4 are conformed the standard specifications of ASTM to be used as a mineral admixture for cement pastes, mortars or even concretes [33-35]. The relationship between the surface area of the OPC and the various cement batches incorporated BA is represented in Figure 4. It is clear that as the BA content increased in the cement mix, the surface area or fineness of the whole mix increased too as shown in Table 3 and Figure 4.

**Table 4** The physical properties of the OPC and BA samples

Property	Kb	Hm	Sm	Am	Lm	Density, $\text{g}/\text{cm}^3$	Blaine Fineness, $\text{cm}^2/\text{g}$	Specific gravity
OPC	2.4419	2.1029	2.9918	1.3111	90.2232	2,8532	3400	3.14
BA	0.1046	0.0863	8.0600	3.6974	3.3145	1.8761	6500	2.23

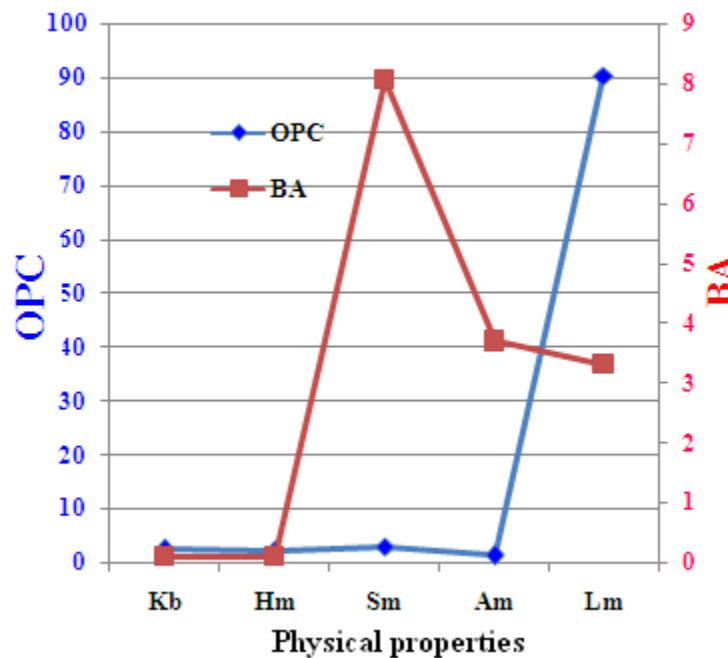


**Figure 2** Physical properties of both OPC and BA samples (Kb: Basicity coefficient, Hm: Hydration modulus, Sm: Silica modulus, Am: Alumina modulus, Lm: Lime modulus)

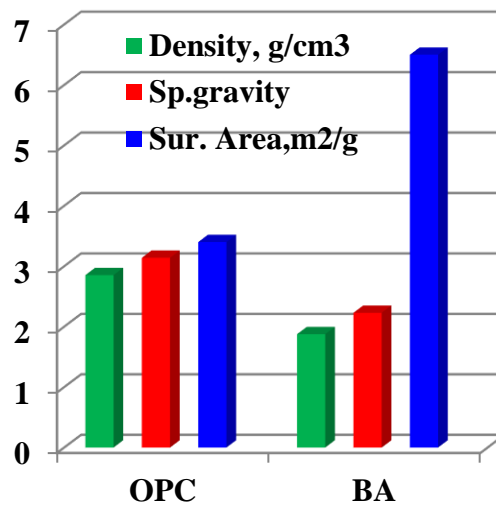


**Figure 3** Relationship between specific gravity, density and surface area of OPC and BA samples.

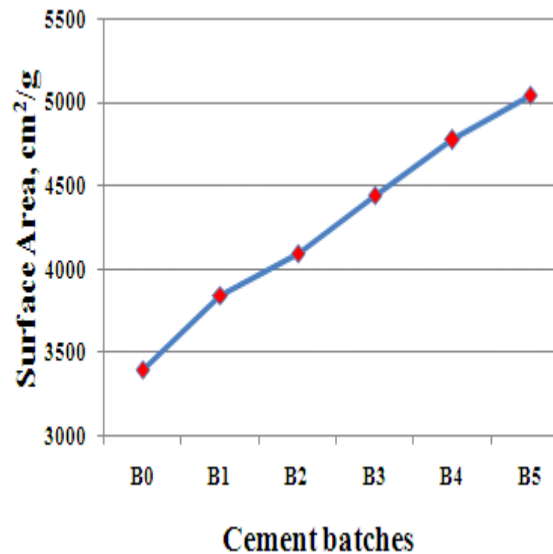


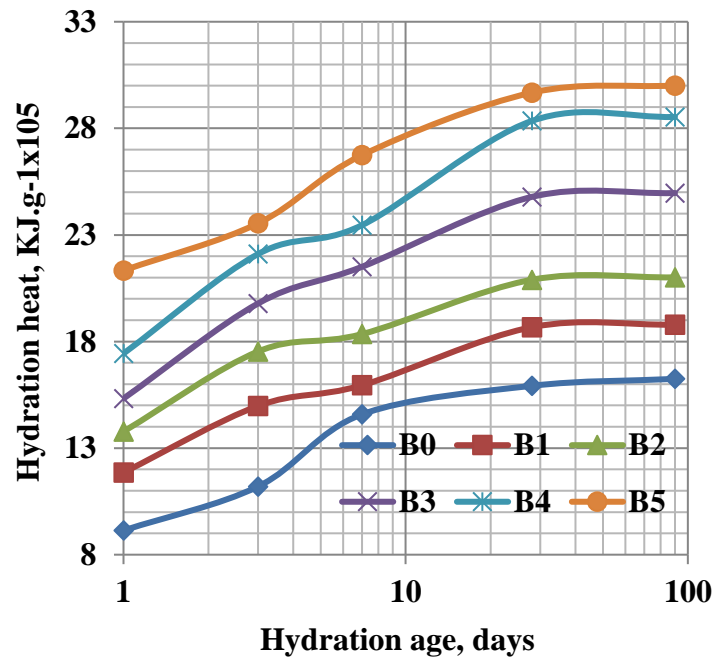
**Figure 4** Relationship between the surface areas of the different cement batches containing BA.

The loss on ignition (LOI) of BA is high (6.81%), which seems to be close to the limit of 10 % specified by ASTM C 618 for pozzolana [36]. However, LOI of BA tends to decrease when the calcination temperature increases. Ganesan et al. [37] used BA with LOI of 4.9% and found that this did not significantly affect the compressive strength of the concrete. However, effects of LOI of BA on the properties of concrete have not been published up till now.

### Heat of hydration

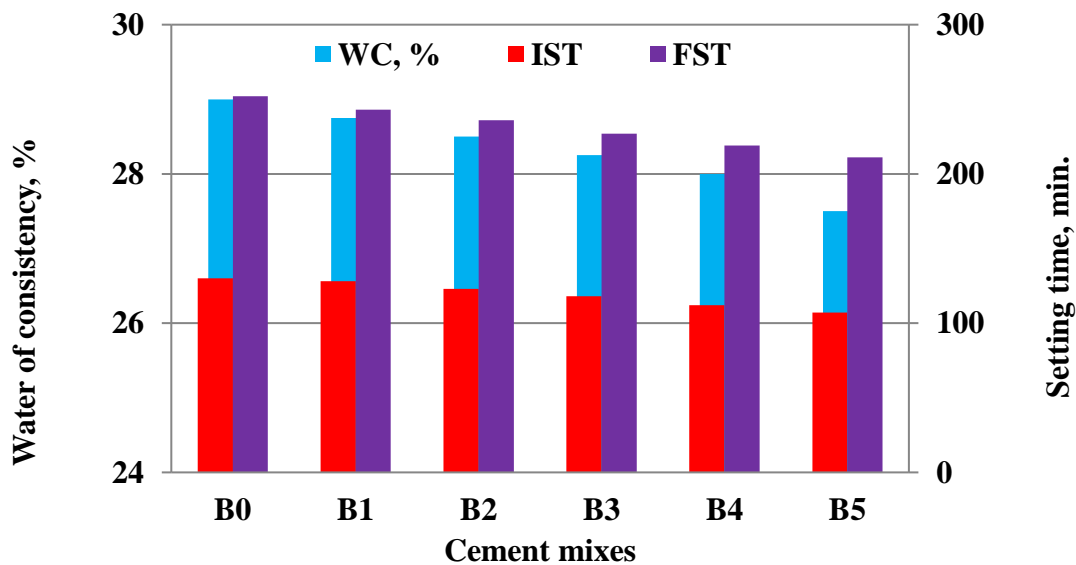
The heat of hydration of the various cement pastes containing BA is graphically represented as a function of curing times for 1, 3, 7, 28 and 90 days in Figure 5. Results illustrated that the heat of hydration of all cement pastes increased as the curing time proceeded up to 90 days which was the same trend for all hardened cement pastes. This is mainly due to the increase of the rate of hydration of cement paste, which is followed by the release of heat. Moreover, the rate of the released heat of hydration enhanced at early ages up to 7 days as the BA content increased. This is essentially attributed to the fact that the fine BA particles activated the hydration reaction mechanism of C<sub>3</sub>S and β-C<sub>2</sub>S. At later ages (28-90 days), the rate of hydration reaction as well as the evolved heat of

hydration also increased, but it is due to the activation effect of the fine BA particles on hydration mechanism of  $\beta$ -C<sub>2</sub>S [17,18]. In a general sense, as soon as the various cement powders become in contact with water, there is a rapid increase in their electrical conductivity values. The variation of electrical conductivity of the BA-cement pastes (B1-B7) shows a similar trend, but with lower values than that of blank (B0) due to the dilution effect of the OPC and/or the retardation effect of BA.



**Figure 5** The heat of hydration of the various cement pastes containing BA hydrated up to 90 days.

#### Water of consistency and setting time



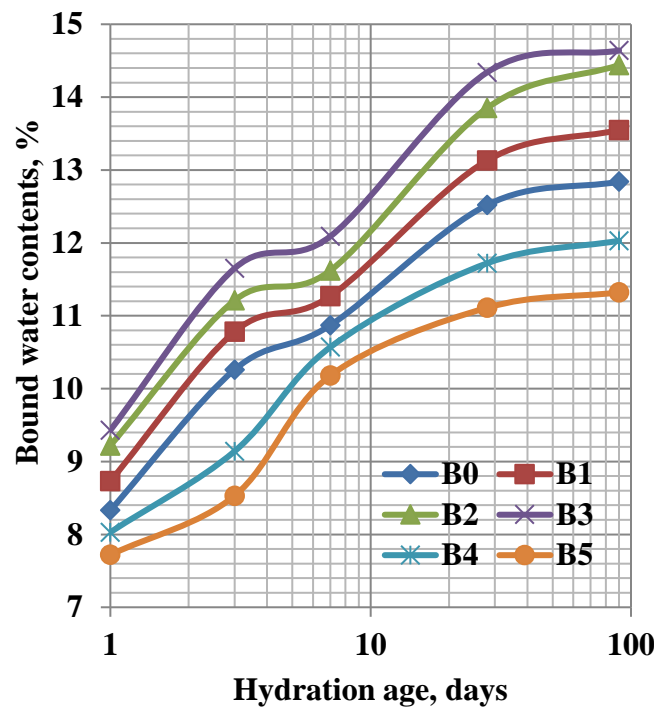
**Figure 6** Water of consistency and setting time of cement blends containing BA cured up to 90 days.

Figure 6 illustrates water of consistency and setting times (Initial and final) of the various cement pastes containing BA (B0-B5). Water of consistency of the various cement pastes were slightly decreased with the increase of BA content. Although the addition of

BA increases the fineness of the whole mix if compared with that of the blank (B0) which in turn tends to increase the w/c ratio, the water of consistency was decreased. On the other side, the initial and final setting times also decreased with increasing BA content. This is essentially attributed to the incorporation of Na-lignosulphonate admixture which is a major superplasticizer, i.e. it tends to largely decrease the w/c ratio [38, 39]. The data obtained are not the same as obtained in other researches [17, 18, 21-23] due to the absence of the used superplasticizer. As a result, it can be concluded that the BA acts as an accelerator in presence of any superplasticizer.

### Chemically-combined water contents

The chemically combined water contents of the different cement pastes containing BA is shown in Figure 7. The combined water content increased as the curing time proceeded up to 90 days. This is principally contributed to the hydration of the main cement phases, especially  $C_3S$ ,  $C_3A$  and  $C_4AF$  at early ages of hydration up to 7 days, whereas  $\beta$ - $C_2S$  often hydrates at later ages from 28 days onward [7,17,18]. The combined water contents slightly increased as the BA content increased up to 12 % and then suddenly decreased sharply with further increase of BA almost at all curing ages, i.e. the cement blends B1, B2 and B3 are slightly higher than that of the blank OPC (B0). This is primarily due to the pozzolanic reactivity of BA through which the constituents of BA can react with the  $Ca(OH)_2$  resulting from the hydration of  $C_3S$  at early stages of hydration and  $\beta$ - $C_2S$  at later stages to produce additional CSH. Whereas, the bound water contents of B4 and B5 are becoming lower comparing with the control mix (B0). The lower values of combined water also may be due to the unburned carbon existed in BA and to the dilution of BA [17, 20-24, 40-44]. Accordingly, it can be concluded that the optimum addition of BA does not exceed 12 % because the higher amounts of BA is undesirable due to its adverse effect, i.e. the higher quantity of BA must be avoided because it may hinder the hydration of cement phases.

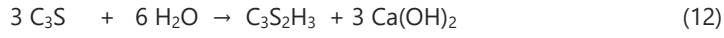


**Figure 7** Chemically bound water contents of cement blends containing BA cured up to 90 days.

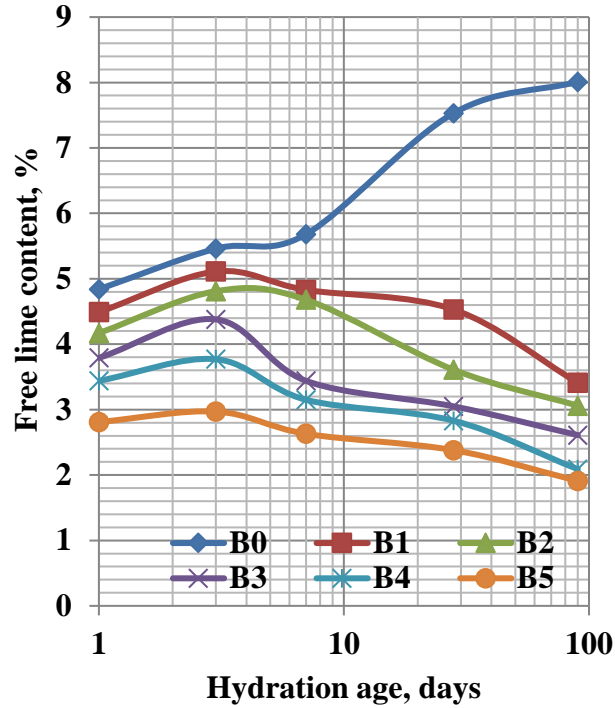
### Free lime contents

Figure 8 indicates the free lime contents of the various cement mixes containing BA hydrated up to 90 days. The free lime contents of B0 gradually increased with the hydration ages indicating an enhancement in the rate of hydration [17, 18]. As the addition of BA increased, the values of free lime are decreased onward and be lower than that of the blank mix (B0) with all cement mixes up to 25 % BA. For mixes B1-B5, the free lime contents increased only up to 3 days and then decreased. The increase is due to the normal hydration while the decrease is due to the pozzolanic reactions between the active nanosilica of BA and the resulting  $Ca(OH)_2$  coming from the hydration of  $C_3S$  at early ages and  $\beta$ - $C_2S$  at later ages of hydration as follows:-





The obtained results proved that the BA acts as a pozzolanic material, and therefore the higher the amount of BA, the higher is the pozzolanic reactivity [40-45].



**Figure 8** Free lime contents of cement blends containing BA cured up to 90 days.

#### Bulk density and apparent porosity

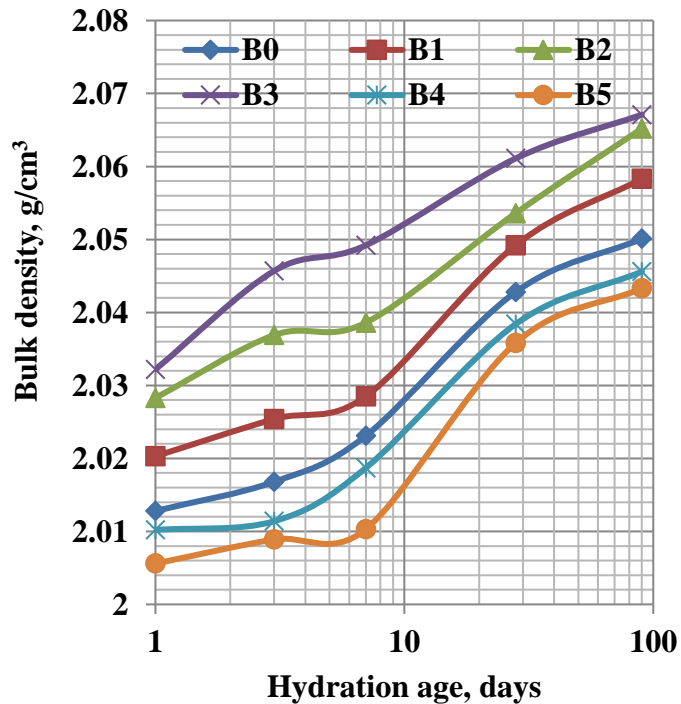


**Figure 9** Bulk density of cement blends containing BA cured up to 90 days.

Figures 9 and 10 demonstrate graphs of the bulk density and apparent porosity of the various cement pastes versus the time of curing. Generally, the bulk density of the various cement mixes increased as the curing time progressed up to 90 days while the apparent porosity decreased. This is mainly contributed to that as curing time proceeds the hydration process begins producing CSH which soon deposited in the pore volume leading to a decrease in the porosity. This reflected positively on the bulk density, i.e. the bulk density increased while the apparent porosity decreased [17, 18, 46]. The bulk density of the various cement mixes containing BA gradually increased as the BA content increased up to 15 %, whereas the apparent porosity decreased, i.e. the cement blends B1, B2 and B3 are slightly higher than that of the of the plain OPC (B0). This is evidently due to the formation of additional CSH from the pozzolanic reactions of BA with the constituents of cement through which the constituents of BA can react with the  $\text{Ca(OH)}_2$  resulting from the hydration of  $\text{C}_3\text{S}$  at early stages of hydration and  $\beta\text{-C}_2\text{S}$  at later stages to produce additional CSH [7,19-21]. With the addition of more than 12 % BA, the BD suddenly decreased while the apparent porosity increased also at all curing ages. This is principally due to the decrease in the main binding material of the OPC and also the higher quantity of BA may obstruct and hinder the hydration process, i.e. it affects negatively and decreases the rate of hydration accompanied by a decrease of BD [7, 18, 20, 26, 32, 41]. Hence, the increase of apparent porosity and the decrease of BD resulted with the incorporation of large amounts of BA affected the amount of the used OPC. As a result, it was not sufficient for inducing the reaction with silica from BA.

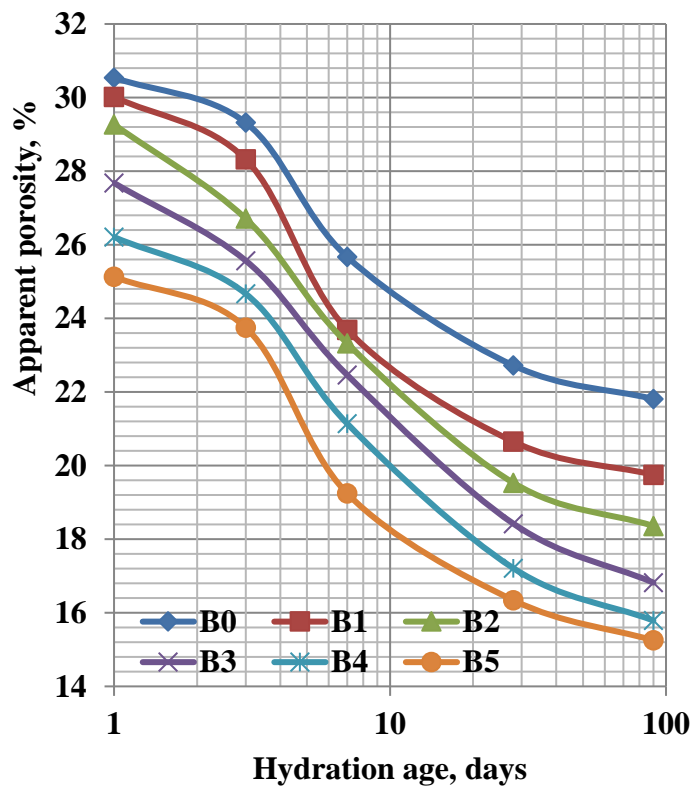
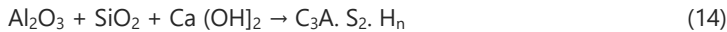


**Figure 10** Apparent porosity of cement blends containing BA cured up to 90 days.

### Compressive strength

It is well known that the w/c ratio of cement pastes and/or concrete affects the workability, which in turn affects the strength of cement pastes and/or concrete, i.e. the decrease of w/c-ratio results in an increase of workability accompanied by an increase in the strength of the hardened cement pastes and/or concrete and the opposite is right. Figure 11 represents the graphs of the compressive strength (CS) of the various cement pastes versus the time of curing up to 90 days. In a general sense, the compressive strength gradually increased as the hydration periods enhanced until reach 90 days. This is mainly attributed to the formation of CSH and/or CAH that precipitated into the pore structure. This results in a decrease in the pore system and an increase in the bulk density. This improved and enhanced the compaction of the prepared samples, besides the good dispersion by the used admixture and the good compaction during casting which in turn reflected positively on the compressive strength, As a result, the compressive strength increased [24, 26, 31, 47]. The CS also enhanced as the BA content increased at all curing ages of hydration. This is

essentially due to the formation of additional CSH that is resulting from the pozzolanic reactions of nanosilica (Nano-SiO<sub>2</sub>) and nanoalumina (Nano-Al<sub>2</sub>O<sub>3</sub>) from BA with the free lime evolved from the hydration of C<sub>3</sub>S and β-C<sub>2</sub>S of cement to produce cubic crystals of hydrogarnet (C<sub>3</sub>A. S<sub>2</sub>. H<sub>n</sub>) as follows:-



The decrease of free lime improves the physicochemical and mechanical properties of the hardened cement pastes and therefore the CS improved and enhanced [31, 32, 34, 48]. Moreover, the decrease of w/c ratio than normal due to the presence of Na-lignosulphonate (Figure 11) results in an improvement in the physical and mechanical strength of the hardened cube samples. The CS also increased as the BA content increased only up to 12 % and then suddenly decreased. The increase of CS is related to the pozzolanic action of BA, while the decrease is due to the fact that the replacing of BA at the expense of the essential cementitious material of the cement and on the other side the higher amount of BA stands as an obstacle against the normal hydration of cement phases. So, the rate of hydration declined and accordingly, this should be reflected negatively on the CS [34-37]. Also, this would be led to the segmentation of large capillary pores and nucleation sites due to the continuous deposition of hydration products (CSH from the normal hydration of cement phases and additional CSH from the pozzolanic reactions of BA with the released free lime [37, 42, 46-49]. The cement mix (B3 recorded the highest values of CS whereas that of B5 exhibited the lowest. On this basis, the cement batch containing 12 % BA is the optimum mix. Hence, the BA does not only improve the various characteristics of the OPC, but from an economical point of view, it also reduces the cost of the very expensive OPC production

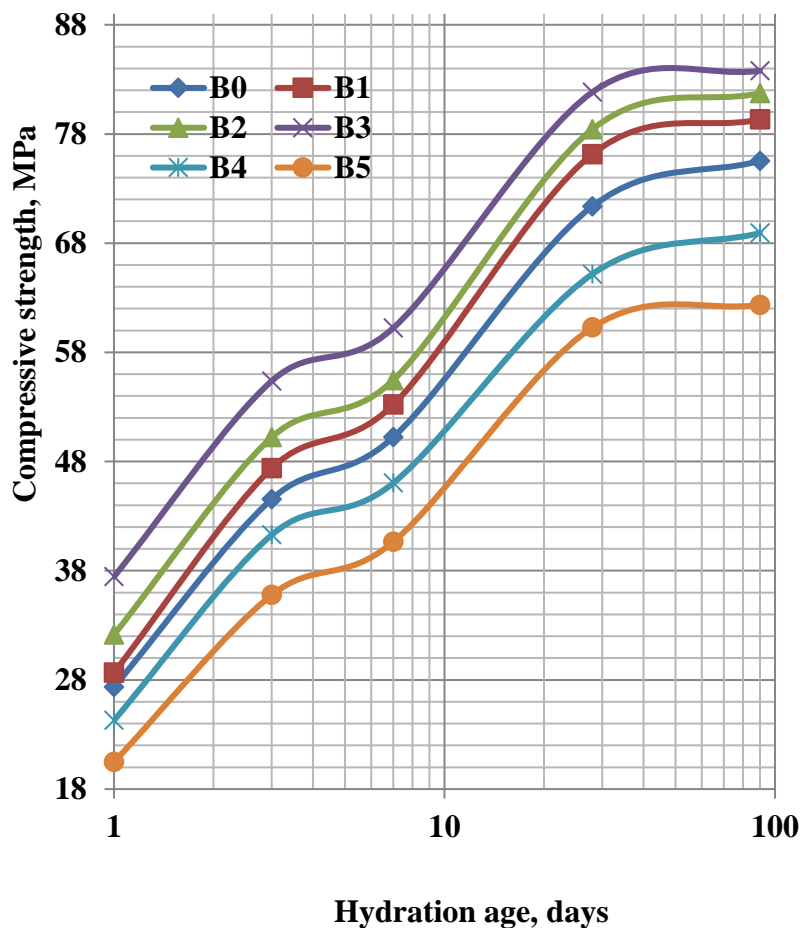


**Figure 11** Compressive strength of cement blends containing BA cured up to 90 days.

### Infrared spectra

The FT-IR spectra of the OPC (B0) and the various OPC cement pastes containing BA (B1-B5) hydrated up to 28 days are shown in Figure 12. Generally, the absorption band at wave number  $3646\text{ cm}^{-1}$  is related to the  $\text{OH}^-$  group coordinated to  $\text{Ca}^{2+}$  that is characterizing the free lime,  $\text{Ca}(\text{OH})_2$  which clearly decreased as BA content increased till gradually disappeared with B5. This is responsible for the improvement of Physical, chemical properties and in particular the compressive strength. The broad absorption band at wave number  $3411\text{ cm}^{-1}$  is due to the  $\text{OH}^-$  group associated to  $\text{H}^+$  bond, i.e. the symmetrical stretching frequency of water. The two absorption bands at  $1796\text{--}1800$  and  $1421\text{--}1432\text{ cm}^{-1}$  which are characterizing to  $\text{CO}_3^{2-}$  and  $\text{SO}_4^{2-}$ , respectively which are due to carbonation and sulphonation of CSH and /or CASH where the vibrations of  $\text{CO}_3^{2-}$  are smaller than those of  $\text{SO}_4^{2-}$ . The three superimposed absorption bands at wave number  $1327\text{ cm}^{-1}$  which are related to  $\text{SO}_4^{2-}$  ions, the main silicate band involve Si-O stretching vibration bands of CSH and the band at  $875\text{--}878\text{ cm}^{-1}$  is due to CASH, respectively. These bands are variable due to the degree of the hydration as well as crystallization. It is clear that the intensity of all absorption spectra were higher in sample B3 containing 12 % BA comparing with the blank (L0) and other mixes.

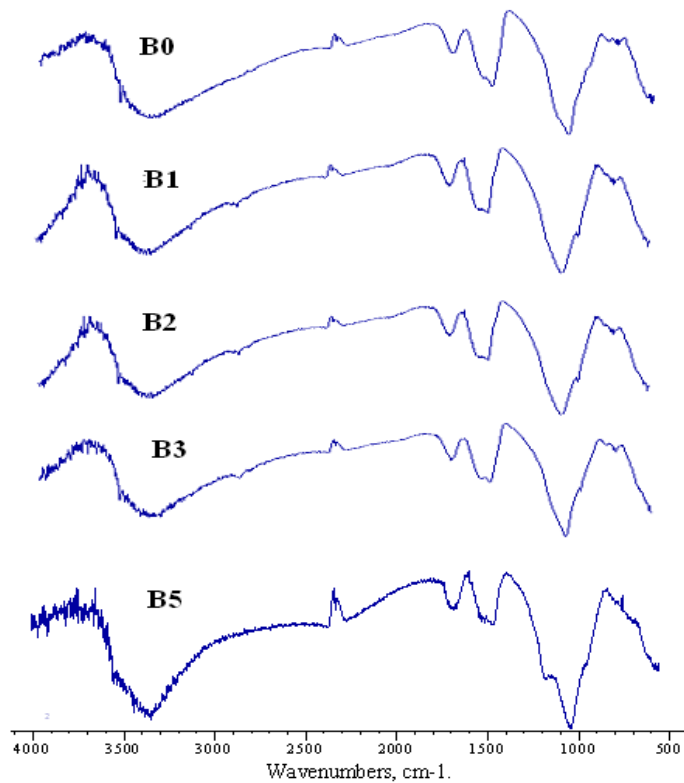


**Figure 12** The FTIR spectroscopy of B0, B1, B2, B3 and B5 hydrated up to 28 days.

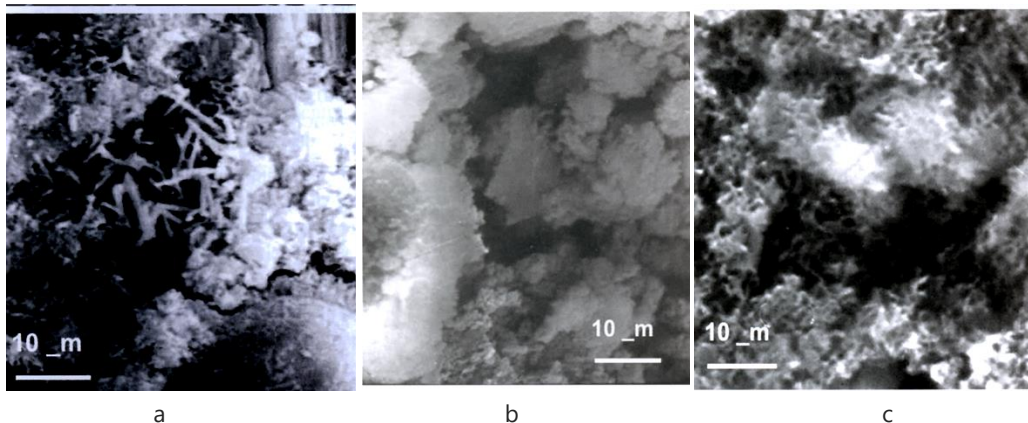


**Figure 13** The SEM microscopy of Portland cement blended with BA hydrated up to 28 days (a-formation of ettringite phase, b-Sheets of CSH and c-Aggregates of CSH).

### SEM microscopy

The SEM microscopy of B0 (a), B3 (b) and B5 (B5 hydrated up to 28 days is shown in Figure 13. The ettringite phase is clearly detected in (B0), sheets of CSH is formed with B3 (b), whereas a porous structure and aggregates of CSH are seen with B3 (c). In addition, spots of free lime are detected in all samples with variable rates.

## 4. CONCLUSIONS

Concerning the findings of the laboratory test results, the following overall conclusions could be obtained:-

1. The heat of hydration increased gradually with the addition of BA at the expense of the cement.
2. The water of consistency (i.e. w/c ratio) as well as setting times (initial and final) are diminished due to the presence of Na-lignosulphonate admixture which it is a superplasticizer that tends to decrease largely the mixing water.
3. The chemically bound water contents increased with the increase of BA only up to 12 % (B3), but then, decreased with the further increase of BA. On contrast, the free lime content increased only up to 3 days and then decreased onward (B1-B5), except that of the blank (B0) which increased continuously up to 90 days.
4. The bulk density improved and enhanced as the BA increased up to 12 % (B3) and then decreased up to 20 % BA. On contrast, the apparent porosity diminished with the replacing up to 12 % BA (B3), and then raised and enhanced onward.
5. The compressive strength significantly improved gradually with increasing the BA content only up to 12 % (B3), and then diminished at all curing ages of hydration. The increase could be done by increasing the pozzolanic reactions that leading to reduce  $\text{Ca}(\text{OH})_2$  which is coming from the hydration of  $\text{C}_3\text{S}$  and  $\beta\text{-C}_2\text{S}$  phases of the cement, and by enhancing the precipitation sites of hydration products and.
6. The addition of 12 % BA (B3) to Portland cement could be applied without any adverse effects on the physicochemical and mechanical properties of Portland cement, but on contrast, and therefore it was selected to be the optimum mix.
7. The FTIR spectra showed the free lime content at the wave length  $3646\text{ cm}^{-1}$  decreased with the increase of BA content.
8. The SEM microscopy indicated that the ettringite phase,  $\text{C}_3\text{A}\cdot 3\text{CaSO}_4\cdot 32\text{H}_2\text{O}$  is formed due to the hydration of  $\text{C}_3\text{A}$  with gypsum in presence of water.
9. The incorporation of the Na-lignosulphonate admixture is the main cause that responsible for the modification and improving most of the physical, chemical, mechanical and microstructure of the hardened cement pastes.

### Acknowledgements

Authors wish to express their deep thanks for NRC for helping to obtain materials, processing, preparing, molding and measuring all of the obtained data of the study, and moreover for financial assistance.

**Funding:** Funded by National Research Centre, Cairo, Egypt.

**Conflicts of Interest:** The authors declare no conflict of interest.

## REFERENCE

1. Ganesan, K.; Rajagopal, K.; Thangavel, K. (2007), Evaluation of bagasse ash as supplementary cementitious material, *Cem. Concr. Comp.*, 29, 515-524.
2. Shih, J.Y.; Chang, T.P.; Hsiao, T.C. (2006). Effect of nanosilica on characterization of Portland cement composite, *Materials Science and Engineering: A*, 424, 266-274.
3. Cordeiro, G.C.; Toledo Filho, R.D.; Tavares, L.M.; Fairbairn, E.M.R. (2008), Pozzolanic activity and filler effect of sugarcane bagasse ash in Portland cement and lime mortars, *Cem. Concr. Comp.*, 30, 410-418.
4. Chusilp, N.; Jaturapitakkul, C.; Kiattikomol, K. (2009), Utilization of bagasse ash as a pozzolanic material in concrete, *Constr. Build. Mater.* 23, 3352-3358.
5. Akram, T.; Memon, S.A.; Obaid, H. (2009), Production of low cost self compacting concrete using bagasse ash, *Constr. Build. Mater.* 23, 703-712.
6. Felekoğlu, B.; Türkel, S.; Baradan, B. (2007), Effect of water/cement ratio on the fresh and hardened properties of self-compacting concrete, *Building and Environment*, 42, 1795-1802.
7. Darweesh, H.H.M.; Abo El-Suoud, M.R. (2017), Saw dust ash substitution for cement pastes-Part I, *Amer. J. Constr. Build. Materials*, 2, 1, 1-9.
8. Abdulkadir, T.S.; Oyejobi, D.O.; Lawal, A.A. (2014), *Evaluation of Sugarcane Bagasse Ash as a Replacement for Cement in Concrete*, *Works Acta Tehnica Corviniensis – Bulletin of Engineering* (Ilorin: University of Ilorin), 71-76.

9. Barroso, J.; Barreras, F.; Amaveda, H.; Lozano, A. (2003), on the optimization of boiler efficiency using bagasse as fuel, *Fuel* 82 1451–63.
10. Senff, L.; Labrincha, J.A.; Ferreira, V.M.; Hotza, D.; Repette, W.L. (2009), Effect of nano-silica on rheology and fresh properties of cement pastes and mortars, *Constr. Build. Mater*, 23, 2487–2491.
11. Singh, N.B.; Singh, V.D.; Rai, S. (2000), Hydration of bagasse ash-blended portland cement, *Cem. Concr. Res.*, 30, 1485–1488.
12. Idris, M.K.; Eldin, K.; Yassin, E. (2015), Determination of the effects of bagasse ash on the properties of Portland cement, *Journal of Appl. and Industr. Sci.*, 3 6–11.
13. Jayminkumar, A.P.; Raijiwala, D.B. (2015), Experimental studies on strength of RC concrete by partially replacing cement with sugar cane bagasse ash, *Int J of Innovative Research in Science, Engineering and Technology*, 4, 2228–2232.
14. Paya, J.; Monzo, J.; Borrachero, M.V.; Diaz Pinzon, L.; Ordonez, L.M. (2007), Sugar-cane bagasse ash (SCBA): Studies on its properties for reusing in concrete production, *Chem. Techn. and Biotechn.*, 77, 2–32.
15. Mangi, S.A.; Jamaluddin, N.; Wan Ibrahim, M.H.; Noridah, M.; Sohu, S. (2017), Utilization of sawdust ash as cement replacement for the concrete production, A review, *Engineering Science and Technology In. Research J*, 1, 11–15.
16. Kawade, U.R.; Rathi, V.R.; Vaishali, D.G. (2013), Effect of sugarcane bagasse ash on strength properties of concrete, *Int J of Innovative Resarch. in Science, Engineering and Techology*, 2, 159–164.
17. Neville, A.M. (2011), "Properties of Concrete", 5<sup>th</sup> Edn, Longman Essex (UK), ISBN: 978-0-273-75580-7 (pbk.).
18. Hewlett, P.C. (2004), Lea's chemistry of cement and concrete, 5<sup>th</sup> edn, Oxford: Elsevier Science & Technology Books. ISBN: 0470 24416 X (Wiley).
19. Aigbodion, V.S.; Hassan, S.B.; Ause, T.; Nyior, G.B. (2010), Potential utilization of solid waste (bagasse ash), *J of Minerals and Materials Characterization and Engineering*, 9, 67–77.
20. Darweesh, H.H.M.; Abo-El-Suoud, M.R. (2015), Quaternary Cement Composites Containing Some Industrial By-products to Avoid the Environmental Pollution, *EC Chemistry*, 2, 1, 78–91.
21. Darweesh, H.H.M. (2017), Mortar Composites Based on Industrial Wastes, *International Journal of Materials Lifetime*, 3, 1, 1–8.
22. ASTM–Standards (1993), Standard Test Method for Normal water of Consistency of Hydraulic Cement, C187-86: 148–150.
23. ASTM –Standards (1993), Standard Test Method for Setting Time of Hydraulic Cement. C191-92: 866–868.
24. Darweesh, H.H.M. (2005), Effect of the combination of some pozzolanic wastes on the properties of Portland cement pastes. *iiCL'industria italiana del Cemento* 808, 298–311.
25. Darweesh, H.H.M.; Nagieb, A. (2007), Hydration and micro-structure of Portland/Calcined Bentonite Blended Cement Pastes, *Indian Journal of Chemical Technology*, 14 301–307.
26. Darweesh, H.H.M. (2014), Utilization of Perlite Rock in Blended Cement-Part I: Physico mechanical properties, *Direct Research Journal of Chemistry and Material Sciences* 2354–4163.
27. ASTM-Standards (1993), Standard Test Method for Compressive Strength of Dimension Stone, C170-90: 828–830.
28. Kondo, R.; Abo-El-Enein, S.A.; Daimon, M. (1975), kinetics and mechanisn of hydrothermal reaction of Granulated blastfurnace slag, *Bulletin of the chrmmical Society Japan*, 48, 222–226.
29. Karim, M.R.; Zain, M.F.M.; Jamil, M. (2012), Strength of Mortar and Concrete as Influenced by Rice Husk Ash: A Review, *World Applied Sciences Journal*, 19.10, 1501–1513.
30. Agarwal, S.K.; Deepali, G. (2006), Utilization of Industrial Wastes and Unprocessed Micro-Fillers for Making Cost Effective Mortars, *Construction and Building Materials*, 20.10, 999–1004.
31. Darweesh, H.H.M.; Abo El-Suoud, M.R. (2014), Setting, Hardening and Mechanical Properties of Some Cement/Agrowaste Composites - Part I, *American Journal of Mining and Metallurgy*, 2, 2, 32–40.
32. Echart, A.; Ludwig, H.M.; Stark, J. (1995), Hydration of the four main Portland cement clinker phases, *Zement-Kalk-Gips*, 48, 8, 443–452.
33. ASTM-Standards (1978), Standard Specification for Coal Fly Ash and Raw or Calcined Natural Pozzolan for Use in Concrete", C 618-12 a.
34. Darweesh, H.H.M. (2012), Setting, hardening and strength properties of cement pastes with zeolite alone or in combination with slag, *Interceram Intern. (Intern Cer Review)*, Germany, Vol. 1, 52–57.
35. Rukzon, S.; Chindaprasirt, P. (2006), Strength of ternary blended cement mortar containing Portland cement, rice husk ash and fly ash, *J Eng Inst*, 17, 33–37.
36. ASTM-C618: Standard specification for coal fly ash and raw or calcined natural pozzolan for use as a mineral admixture in concrete; 1997; 04.02:294–6.
37. Ye, Q.; Zhang, Z.N.; Kong, D.Y.; Chen, R.S. (2007), Influence of nano-SiO<sub>2</sub> addition on properties of hardened cement paste as compared with silica fume, *Constr. Build. Mater.*, 21, 3, 539–545.

38. Ayoub, M.M.H.; Darweesh, H.H.; Negim, S.M. (2008), "Utilization of hydrophilic copolymers as super-plasticizers for cement pastes" *Cem. Hormigon, Spain*, 2008, 910, 4-15.
39. Darweesh, H.H.M. (2014), Utilization of Ca-lignosulphonate prepared from black liquor waste as a cement superplasticizer, *J. Chemistry and Materials Research*, Vol., 1, No. 2, 28 -34
40. Heikal, M.; Ali, A.I.; Ismail, M.N.; Awad, S.; Ibrahim, N.S. (2014), Behavior of composite cement pastes containing silica nano-particles at elevated temperature, *Const. Build. Mater.*, 70. 339-350.
41. Amin, M.; Abu El-Hassan, K. (2015), Effect of using different types of nano materials on mechanical properties of high strength concrete, *Constr. Build. Mater.*, 80, 116–124.
42. Stefanidou, M.; Papayianni, I. (2012), Influence of nano-SiO<sub>2</sub> on the Portland cement pastes, *Compos. Part B-Eng.* 43, 2706–2710.
43. Nazari A, Riahi S; Riahi S; Shamekhi SF; Khademno A (2010), Influence of Al<sub>2</sub>O<sub>3</sub> nanoparticles on the compressive strength and workability of blended concrete, *Journal of American Science*, 6, 6-9.
44. Ibrahim, N.S.; Heikal, M.; Ismail, M.N. (2015), Physico-mechanical, microstructure characteristics and fire resistance of cement pastes containing Al<sub>2</sub>O<sub>3</sub> nano-particles, *Const. Build. Mater.*, 91, 232-242.
45. Givi, A.N.; Rashid, S.A.; Aziz, F.N.A.; Salleh, M.A.M. (2010), Experimental investigation of the size effects of SiO<sub>2</sub> nanoparticles on the mechanical properties of binary blended concrete, *Composites Part B: Engineering*, 41, 673-677.
46. Nazari, A.; Riahi, S. (2011), The effects of SiO<sub>2</sub> nanoparticles on physical and mechanical properties of high strength compacting concrete, *Compos. Part B-Eng.* 42, 570–578.
47. Aleem, S.A.E.; Heikal, M.; Morsi, W.M. (2015), Hydration characteristic, thermal expansion and microstructure of cement containing nano-silica ,*Const. Buil. Mater.*, 59. 151-160.
48. Nazari, A.; Riahi, S. (2011), The effects of SiO<sub>2</sub> nanoparticles on physical and mechanical properties of high strength compacting concrete. *Composites Part B: Engineering*, 42, 570-578.
49. Ren, J.; Lai, Y.; Gao, J. (2018), Exploring the influence of SiO<sub>2</sub> and TiO<sub>2</sub> nanoparticles on the mechanical properties of concrete, *Constr. Build. Mater*, 175, 277–285.